



# Green synthesis of Cu/zirconium silicate nanocomposite by using *Rubia tinctorum* leaf extract and its application in the preparation of *N*-benzyl-*N*-arylcyanamides

Mahmoud Nasrollahzadeh<sup>1</sup> | Mohaddeseh Sajjadi<sup>1</sup> | S. Mohammad Sajadi<sup>2</sup>

<sup>1</sup> Department of Chemistry, Faculty of Science, University of Qom, Qom 3716146611, Iran

<sup>2</sup> Department of Petroleum Geoscience, Faculty of Science, Soran University, PO Box 624, Soran, Kurdistan Regional Government, Iraq

## Correspondence

Mahmoud Nasrollahzadeh, Department of Chemistry, Faculty of Science, University of Qom, Qom 3716146611, Iran.  
Email: mahmoudnasr81@gmail.com

A simple and convenient protocol was established for the synthesis of the *N*-benzyl-*N*-arylcyanamides through *N*-benzylation of a wide variety of arylcyanamides using copper nanoparticles immobilized on natural zirconium silicate as a novel and green heterogeneous catalyst. In this study, we showed a novel, cost efficient, convenient and simple method for green synthesis of Cu/zirconium silicate nanocomposite by using *Rubia tinctorum* leaf extract as capping and reducing agent. The structure of the novel catalyst was successfully characterized using a number of micro/spectroscopic techniques such as XRD, FESEM, BET, EDS, TEM, FT-IR and elemental mapping. TEM micrographs of obtaining biocatalyst revealed mostly spherical particles with an average diameter of about 15–25 nm on the surface of natural support. The prepared catalyst was used in the *N*-benzylation of a variety of arylcyanamides with benzyl bromide and showed high activity and stability for the efficient synthesis of *N*-benzylarylcyanamides in good yields. Remarkably, the catalyst can be easily recovered from the reaction medium and reused up to five runs without losing its catalytic activity.

## Highlights

- Preparation of the Cu/zirconium silicate nanocomposite using *Rubia tinctorum* leaf extract.
- The Cu/zirconium silicate nanocomposite was characterized using FT-IR, XRD, BET, FESEM, TEM, XRD, EDS and elemental mapping.
- Synthesis of *N*-alkyl-*N*-arylcyanamides using Cu/zirconium silicate nanocomposite.
- The catalyst can be easily recovered and reused up to five runs without significant loss of catalytic activity.

## KEYWORDS

Cu/zirconium silicate nanocomposite, Cyanamides, Heterogeneous catalyst, *N*-benzyl-*N*-arylcyanamides, *Rubia tinctorum*

## 1 | INTRODUCTION

Cyanamides are important and significant class of reactive organic molecules with a broad range of applications in the organic synthetic and coordination chemistry.<sup>[1–4]</sup>

Cyanamide and its derivatives are versatile nitrogen-carbon-nitrogen (N-C-N) building blocks for the synthesis of not only guanidine-containing molecules, amidines, and other nitrogen-containing compounds but also ambidentate ligands. Besides, cyanamide based compounds are known to have a variety of interesting biological activities such as anticancer<sup>[5]</sup> and antiviral.<sup>[6]</sup>

Cyanamides can be considered as one of the bifunctional molecules because of having nucleophilic amino nitrogen ( $sp^3$ ) atom and an electrophilic nitrile ( $sp$ ) group. The high reactivity and unique structure of the cyanamide units in the different heterocyclizations and complexations (complex preparation) is dependent on lone pair electron on the amino nitrogen atom (nucleophile) and triple-bonded carbon atom (electrophile).

Although, a wide range of monosubstituted cyanamides (RNHCN) are known as valuable dinitrogen resource, there is still a dearth of suitable synthetic procedures for the synthesis of disubstituted cyanamides (RR'NCN).<sup>[2,7–9]</sup> Despite versatile uses of disubstituted cyanamides, only a limited number of their synthetic methods have been reported, especially *N*-alkyl-*N*-arylcyanamides as one of disubstituted cyanamides which received less attention for the lack of convenient and robust methods of their synthesis.<sup>[2,7–9]</sup> Indeed, *N*-alkyl-*N*-arylcyanamides are an important class of reactive organic molecules containing amino and cyano groups that can be broadly used in both organic synthetic and medicinal chemistry. Thus, there is an essential need to develop new and convenient synthetic procedures for the synthesis of *N*-alkyl-*N*-arylcyanamides.

Over the past decade, the use of metal nanoparticles (MNPs) have been developed due to their unique properties such as high catalytic activity, high surface-to-volume

ratio, low toxicity and cost, simple recovery, recyclability, high stability, and insolubility in organic solvents.<sup>[10–13]</sup> Among various metal NPs, Ag,<sup>[14]</sup> Pd,<sup>[15]</sup> Ni,<sup>[16]</sup> Au<sup>[17]</sup> and particularly Cu NPs<sup>[18]</sup> have most commonly been employed as catalyst to catalyze the organic transformations. To date, a various range of heterogeneous catalytic systems *via* the immobilization of metal NPs on suitable solid supports due to the decrease of their agglomeration problem and increase of the efficient organic transformations have been designed, synthesized and developed.<sup>[19–21]</sup> Thus, noble metal NPs immobilized on the solid support surface such as zeolite,<sup>[22]</sup> Fe<sub>3</sub>O<sub>4</sub>,<sup>[23]</sup> SBA-15,<sup>[24]</sup> graphene<sup>[25]</sup> and metal-organic frameworks<sup>[26]</sup> have been applied in the organic catalytic transformations.

Zirconium silicate is well known via a number of applications in different fields such as nuclear reactor components, surface cleaning, food and other medical industries.<sup>[27]</sup> Moreover, zirconium silicate was considered as an adsorbent for the removal of different organic and inorganic pollutants and some heavy metal ions,<sup>[28,29]</sup> but there is no report of its use as a support. Zirconium silicate is generally constructed *via* electric/thermal fusion of the zirconium oxide (ZrO<sub>2</sub>) and silicon oxide (SiO<sub>2</sub>) used as a platform for the immobilization of the diverse MNPs. Zirconium silicate can be used widely as a natural, novel and environmentally benign support to catalyze the organic synthetic transformations for its porous structure, excellent chemical stability, high temperature resistance, inexpensive, low toxicity and very low solubility in different solvents.<sup>[29,30]</sup>

Nowadays, green chemistry approaches encouraged researchers towards the green synthesis of nanoparticles by using biological synthetic methods to avoid the toxic and hazardous substances, organic solvents and use of expensive and toxic reducing agents which commonly used in physicochemical methods.<sup>[31–36]</sup> A large number of MNPs immobilized on solid support surface were successfully synthesized by using different plant extracts as



**FIGURE 1** Image of the *Rubia tinctorum* plant

reducing and capping agents in simple, eco-friendly and cost effective routes against the conventional physical and chemical methods.<sup>[37–40]</sup>

*Rubia tinctorum* from *Rubiaceae* family is a medicinal plant of southern and west Asia used in traditional medicine as antibacterial, antioxidant and anti inflammatory drug (especially its roots and rhizomes) (Figure 1). The results obtained by phytochemical screening for *R. tinctorum* revealed the presence of Alkaloids, Phenol, Cardiac glycosides, Flavonoids, Terpenes, Tanins, Ratenges, Coumarines and Essential oils.<sup>[41–43]</sup> According to the literature surveys the presence of certain bioactive compounds isolated from the roots of *Rubia* such as flavonoid glycosides, anthraquinone derivatives as glycosides (ruberthric acid, lucidin primveroside) and aglycones (alizarin, lucidin, purpurin), 1-hydroxy-2-methyl-9,10-anthraquinone (II), 1,3,6-trihydroxy-2-methyl-9,10-anthraquinone 3-O-(6'-O-acetyl)- $\alpha$ -L-rhamnosyl (1-2)- $\beta$ -D-glucoside (III), 1,3,6-trihydroxy-2-methyl-9,10-anthraquinone-3-O- $\alpha$ -L-rhamnosyl (1-2)- $\beta$ -D-glucoside (IV), 1,3,6-trihydroxy-2-methyl-9,10-anthraquinone-3-O-(6'-O-acetyl)- $\beta$ -D-glucoside (V), 2-carbomethoxy-3-prenyl-1, 4-naphthohydroquinone- $\beta$ -D-glucoside (VI) and rubimallin (VII).<sup>[44–47]</sup>

In continuation of our attempts to develop the novel heterogeneous catalysts based on different plant extracts, herein, the *Rubia tinctorum* leaf extract was used for the preparation of the Cu/zirconium silicate nanocomposite which its catalytic activity was investigated in the *N*-benzylation of wide variety of arylcyanamides with benzyl bromide for the convenient synthesis of *N*-benzylaryl cyanamides in good to excellent yields (Scheme 1). Until now, there is no report on the synthesis of the *N*-benzylaryl cyanamides using biosynthesized Cu/zirconium silicate nanocomposite.

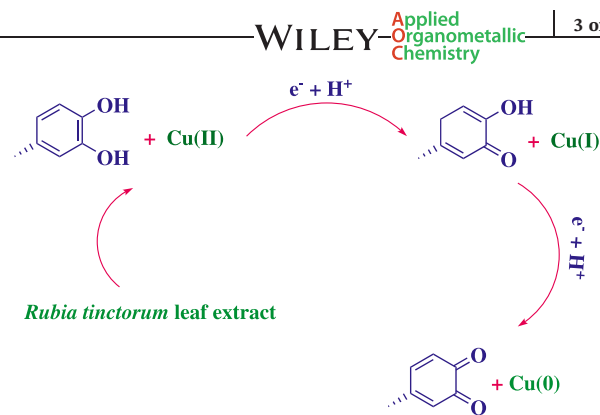
## 2 | RESULTS AND DISCUSSION

### 2.1 | Preparation and characterization of the Cu/zirconium silicate nanocomposite

*Rubia tinctorum* roots and rhizomes have been used in folk medicine for its bioactive constituents. In this work, *Rubia tinctorum* leaf extract was used as an effective reducing and stabilizing agent for the synthesis of metal NPs without addition of any other external reducing



**SCHEME 1** *N*-Benzylation of arylcyanamides using Cu/zirconium silicate nanocomposite



**SCHEME 2** Proposed mechanism for green synthesis of Cu NPs using *Rubia tinctorum* leaf extract

agents. For further monitoring, in a typical synthesis of Cu/zirconium silicate nanocomposite, first Cu nanoparticles were separately synthesized using *Rubia tinctorum* leaf extract. The plant extract composed of compounds with potential antioxidant activity conversion ability of  $\text{Cu}^{2+}$  ions to  $\text{Cu}^0$  (Scheme 2). The preparation of the Cu NPs on the surface of zirconium silicate as an inexpensive and stable support was carried out using the *Rubia tinctorum* leaf extract as capping and stabilizer source.

The UV spectrum of extract (Figure 2) shows bands at 365 nm (band I) and 251 nm (band II) assigned to the cinnamoyl and benzoyl systems of phenolics compounds, Figure 2. As the UV-Vis spectra of monitored NPs showed significant changes in the absorbance maxima due to surface Plasmon resonance of formed Cu NPs. The color of the mixture changed into dark after 6 min at 575 nm indicating the successful green reaction. The nanoparticles obtained by this method are quite stable with no significant variance in the shape, position and symmetry of the absorption peak even after 25 days.

Furthermore, the FT-IR of Cu NPs shows the interaction between  $\text{CuCl}_2 \cdot 2\text{H}_2\text{O}$  and involved sites of

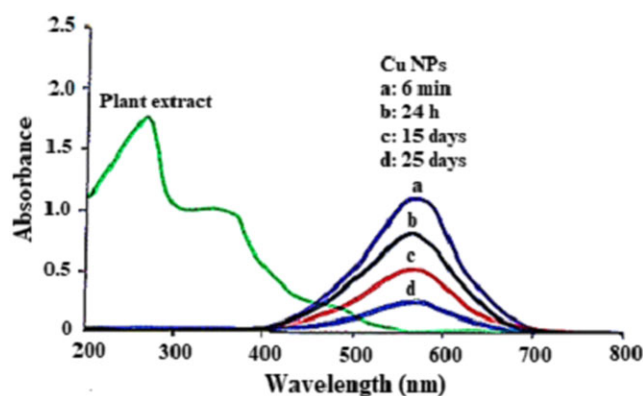


**FIGURE 2** UV-Vis spectrum of the plant extract and green synthesized Cu NPs

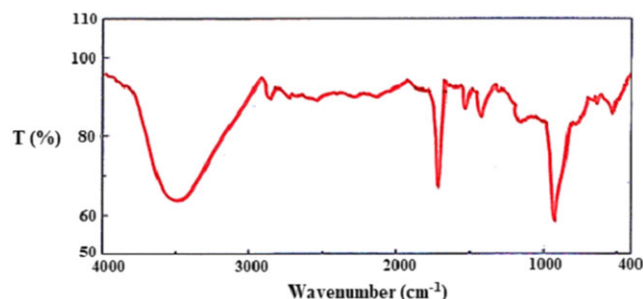


**FIGURE 3** FT-IR spectrum of biosynthesized Cu NPs

phytochemicals to synthesis of Cu NPs. The main peaks at  $3500$ ,  $1715$  and  $1512\text{ cm}^{-1}$  represent the OH functional groups, carbonyl group ( $\text{C}=\text{O}$ ) and stretching  $\text{C}=\text{C}$

aromatic ring vibrations, respectively undergoes the phytochemicals adsorbed on nanosurface (Figure 3).

The green synthesized Cu NPs on the surface of zirconium silicate nanocomposite has been proved using XRD, FT-IR, BET, FESEM, EDX, TEM and elemental mapping characterization methods.

The FT-IR analysis of zirconium silicate and Cu/zirconium silicate nanocomposite are shown in Figure 4a and b, respectively. The analysis has carried out to confirm the constant position of surficial functional groups of the zirconium silicate, even after the immobilization of the Cu NPs in the adsorption process. Figure 4 showed the characteristic bands at around  $3425\text{ cm}^{-1}$  and  $1624\text{ cm}^{-1}$  corresponding to the stretching and bending vibrations of -OH functional

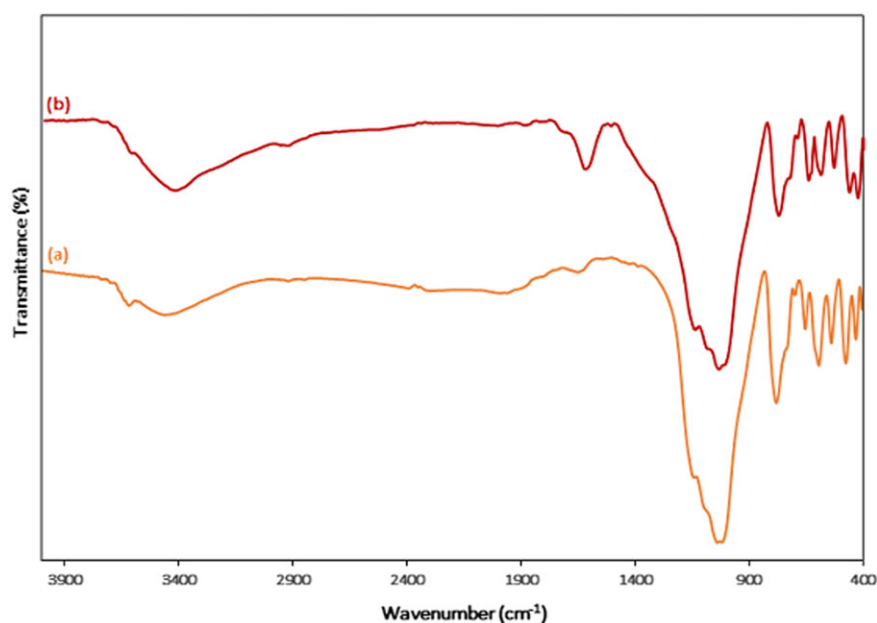


**FIGURE 4** FT-IR spectra of the zirconium silicate (a) and Cu/zirconium silicate nanocomposite (b)

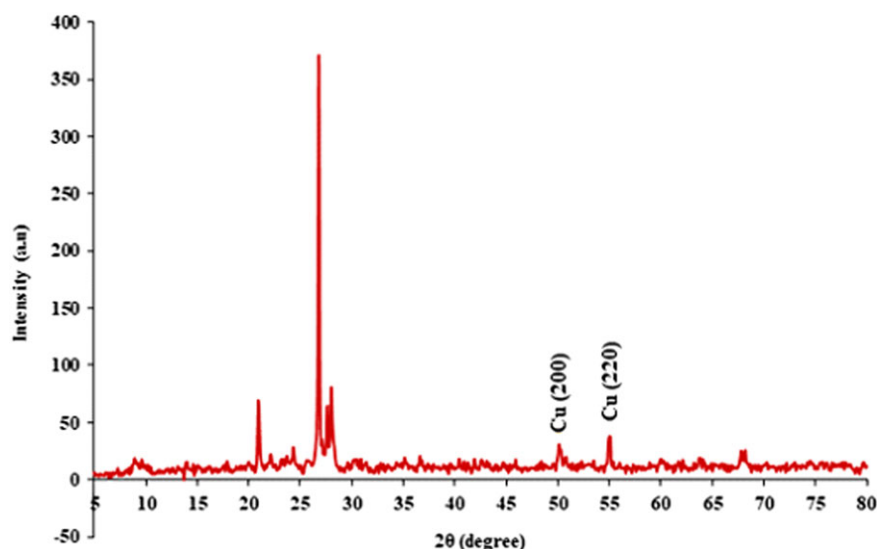


**FIGURE 5** XRD pattern of the biosynthesized Cu/zirconium silicate nanocomposite



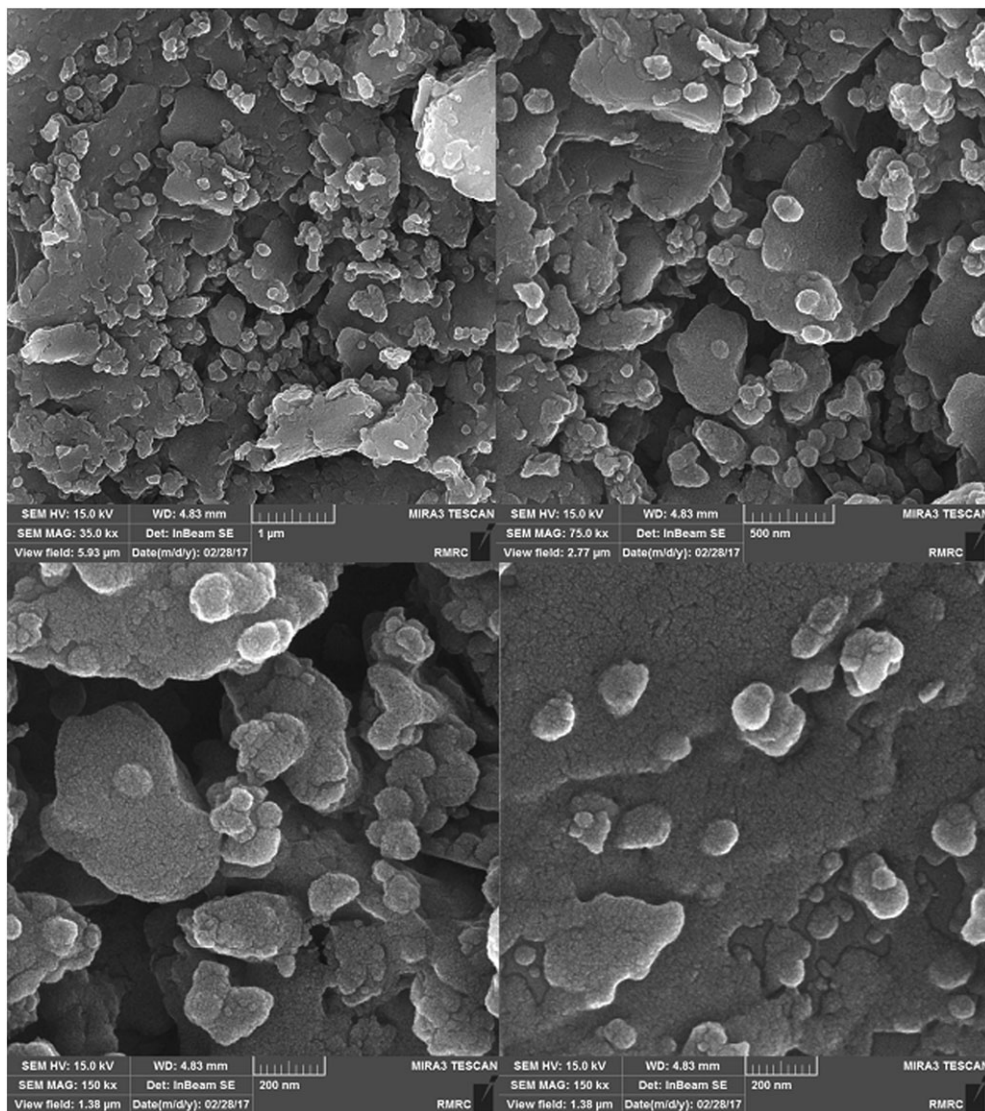


**FIGURE 6** FESEM images of the Cu/zirconium silicate nanocomposite

groups of adsorbed water in the sample, respectively. The characteristic adsorption peaks at about 429–591, 640 and 776  $\text{cm}^{-1}$  were assigned to the metal-oxygen bonding in the Si-O and Zr-O forms.<sup>[28,48]</sup> The absorption bands of the Cu-O bonds have been overlapped by the same frequency regions of Si-O and Zr-O in the natural support.

The crystal structures of the Cu NPs immobilized on zirconium silicate was studied by XRD analysis (Figure 5). In this Figure, sharp and strong peaks at  $2\theta = 21.0, 26.8, 28.7$  and  $55^\circ$  are several characteristic peaks of the matrix of zirconium silicate.<sup>[49]</sup> The observed XRD peaks at  $50.1^\circ$  and  $68.2^\circ$  are assigned to (200) and (220) planes of the face-centered cubic (fcc) Cu crystals, respectively, which are in a good agreement with the reported XRD pattern of Cu NPs (JCPDS No.04–0836).<sup>[50]</sup>

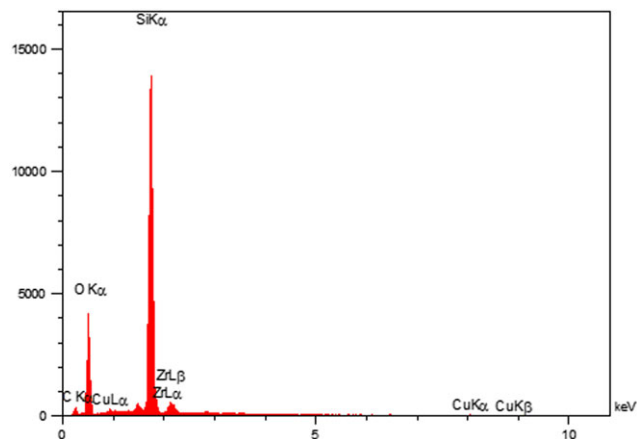


**FIGURE 7** EDS spectrum of the Cu/zirconium silicate nanocomposite

FESEM and TEM analysis were used to study the surface morphology, structure and size of the particles. FESEM images of the biologically synthesized

Cu/zirconium silicate nanocomposite are shown in Figure 6. The micrographs depicted the uniformly distribution of the Cu NPs as spherical particles on the surface

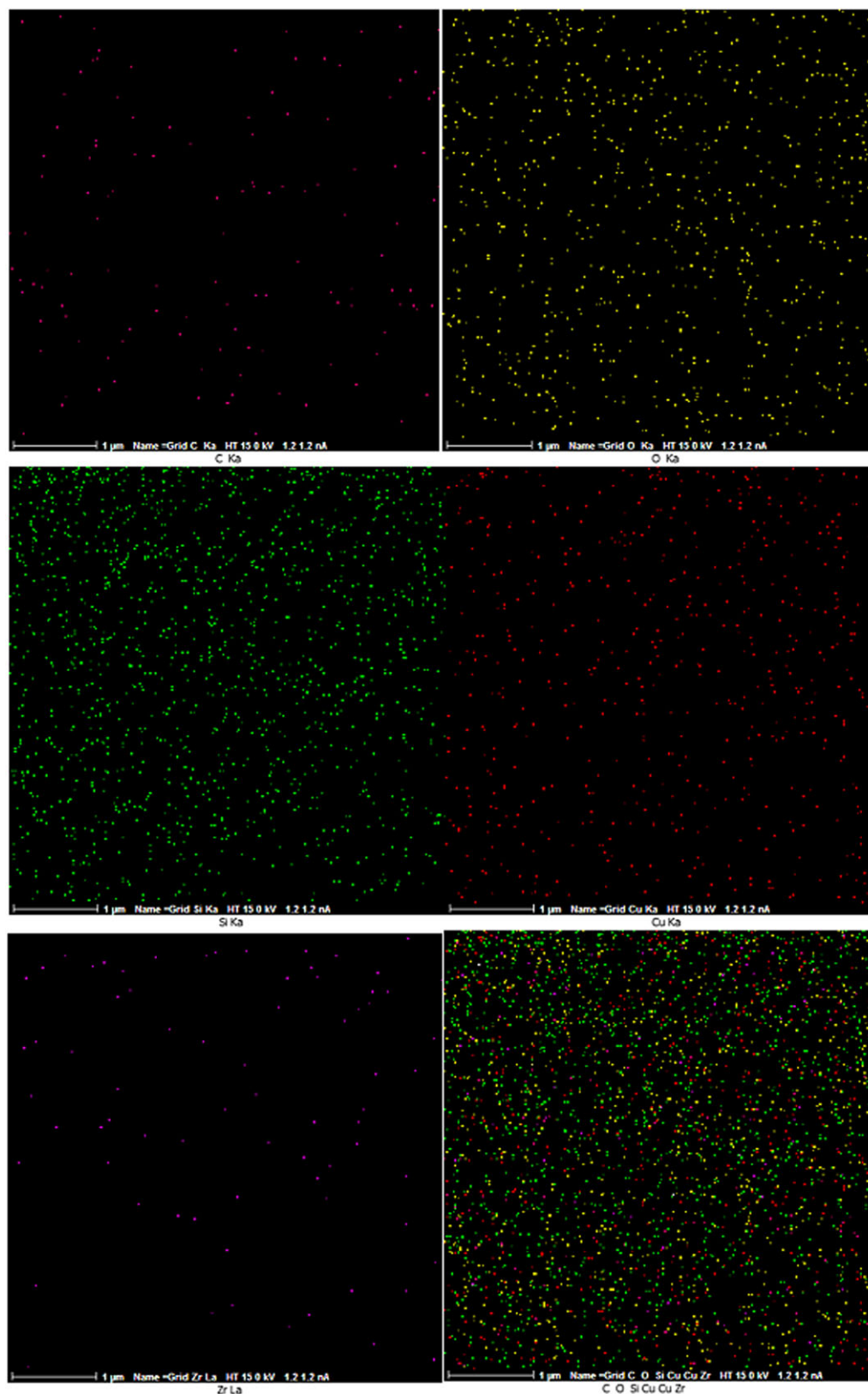


**FIGURE 8** Elemental mapping of the Cu/zirconium silicate nanocomposite

of zirconium silicate matrix with a good combination between this material.

The distributions of the elements in the biosynthesized catalyst were analyzed using EDS spectrum and elemental mapping images. The EDS spectrum can be confirmed the coexistence of Si, O, Zr, C, and Cu elements in the newly Cu/zirconium silicate nanostructure indicating their chemical composition in the catalyst (Figure 7). As shown in Figure 8, the elemental mapping images of the Cu/zirconium silicate nanocomposite were confirmed the distribution of the Cu NPs on the surface of zirconium silicate matrix.

The TEM images of the Cu/zirconium silicate nanocomposite at different magnifications are shown in Figure 9. The obtained nanoparticles are made up of spherical morphology with an identical-nanometer size. Based on the results of the above-mentioned analyses from the prepared catalyst, it is entirely confirmed that Cu NPs were exactly immobilized on the zirconium silicate surface.

The surface area of the Cu/zirconium silicate nanocomposite was determined by BET (Brunauer–Emmett–Teller). The  $N_2$  adsorption–desorption isotherm and Barrett–Joyner–Halenda (BJH) pore size distribution plot of the Cu/zirconium silicate nanocomposite is shown in Figure 10. The BET surface area, average pore diameter and total pore volume of the Cu/zirconium silicate

nanocomposite are  $5.2929 \text{ m}^2 \text{ g}^{-1}$ ,  $25.28 \text{ nm}$  and  $33.447 \times 10^{-3} \text{ cm}^3 \text{ g}^{-1}$ , respectively.

## 2.2 | Preparation of the *N*-benzyl-*N*-arylcyanamides

The catalytic activity of green synthesized Cu/zirconium silicate nanocomposite was evaluated for the synthesis of the *N*-benzyl-*N*-arylcyanamides *via* reaction of arylcyanamides with benzyl bromide.

Initially, we studied the reaction of 4-bromophenylcyanamide with benzyl bromide in the presence of various amount of the Cu/zirconium silicate nanocomposite. The corresponding product (*N*-benzyl-*N*-(4-bromophenyl)cyanamide) was not detected in the absence of catalyst (Table 1, entry 1), even when reaction time was prolonged to 6 hr. Among various solvents tested, MeCN was most effective in the synthesis of the corresponding product. The effect of temperature was also investigated. The control reaction confirmed that the best yields were obtained when reaction was carried out in MeCN at  $75^\circ\text{C}$  in the presence of 0.05 g of the Cu/zirconium silicate nanocomposite (Table 1, entry 4). Nevertheless, longer reaction times were required when reaction was carried out at room temperature or 0.03 g of the catalysts (Table 1, entries 2 and 3).

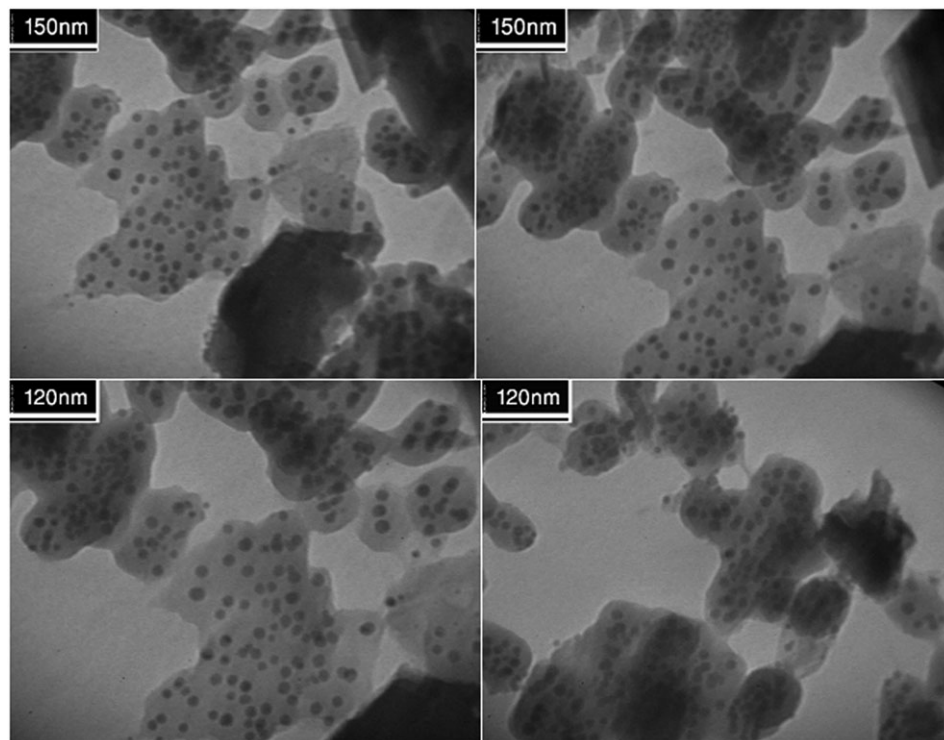


**FIGURE 9** TEM images of the Cu/zirconium silicate nanocomposite



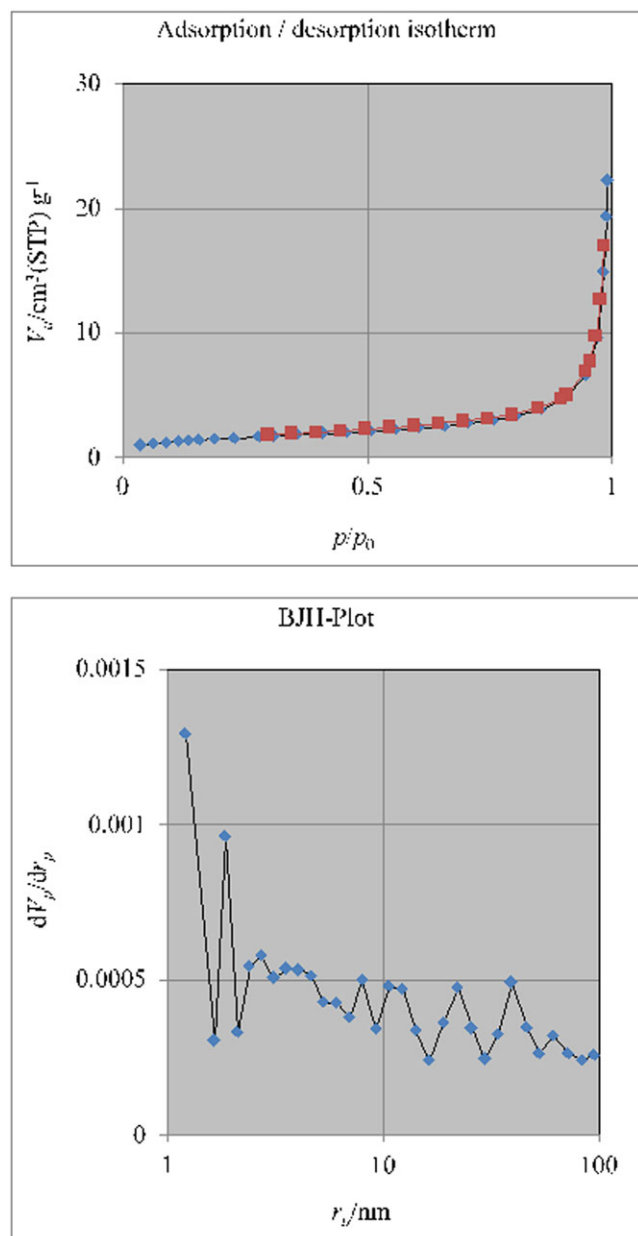


**FIGURE 10** The BET analysis of the Cu/zirconium silicate nanocomposite

With the optimized conditions defined, the *N*-benzylation of various arylcyanamides containing both electron-releasing and electron-withdrawing groups with benzyl bromide was also investigated to study the effects of the substituents. As seen in Table 2, arylcyanamides bearing electron-donating and electron-withdrawing substituents gave corresponding products in good to excellent yields.

The proposed mechanism for the *N*-benzylation of arylcyanamides using Cu/zirconium silicate nanocomposite in MeCN at 75 °C is shown in Scheme 3. The Lewis acidity of the Cu/zirconium silicate nanocomposite probably has an important role in the *N*-benzylation of

**TABLE 1** Optimization of reaction conditions in the preparation of the *N*-benzyl-*N*-(4-bromophenyl)cyanamide

Entry	Catalyst (g)	Solvent	Temperature/ °C	Time	Yield (%)
1	0.0	MeCN	75	6 h	0.0
2	0.03	MeCN	75	175 min	78
3	0.05	MeCN	r.t.	210 min	73
4	0.05	MeCN	75	160 min	87
5	0.05	MeCN	Reflux	160 min	87
6	0.05	EtOH	75	3 h	75
7	0.07	MeCN	75	160 min	87

Reaction conditions: 1.0 equiv of 4-bromophenylcyanamide, 1.0 equiv of benzyl bromide, catalyst and solvent (7.0 ml). Isolated yield.

arylcyanamides. It was proposed that the activation of the C-Br bond of benzyl bromide using Cu/zirconium silicate nanocomposite allows to the formation of *N*-benzyl-*N*-arylcyanamides via an  $S_N2$ -type mechanism in aprotic solvent of MeCN with nucleophilic attack of the arylcyanamides.

After completion of the reaction, the solvent was concentrated and obtained products were purified by recrystallization from EtOH/H<sub>2</sub>O mixture and characterized by melting points, CHN, FT-IR, <sup>1</sup>H NMR and <sup>13</sup>C NMR. Elimination of one strong and sharp absorption band belonged to the NH stretching band in the FT-IR spectrum confirmed formation of the *N*-benzyl-*N*-arylcyanamides. Also, the appearance of one single peak around  $\delta$  4.5–5.5 in the <sup>1</sup>H NMR and 52–58 ppm in the <sup>13</sup>C NMR spectra corresponding to the CH<sub>2</sub> group in *N*-benzyl-*N*-arylcyanamides confirmed the preparation of the product.

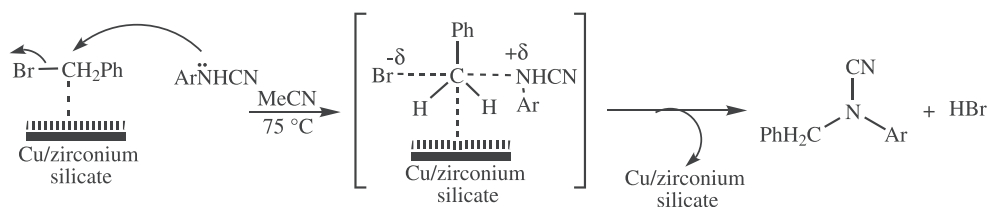
### 3 | CATALYST RECYCLABILITY

The recyclability and reusability of the Cu/zirconium silicate nanocomposite for the synthesis of *N*-benzyl-*N*-arylcyanamides was investigated under the optimized reaction conditions (Figure 11). The recyclability of the novel catalyst can be obtained from the efficient stabilization of the Cu/zirconium silicate. After completion of the *N*-benzylation reaction, the catalyst was isolated by a simple filtration and washed with ethanol and dried to be reused for the next run. According to the recycling process results, the catalyst can be reused five times without any additional activation treatment. Besides, the morphology, size, and structure stability of recycled Cu/zirconium silicate nanocomposite was confirmed by EDS, FESEM and TEM techniques



**TABLE 2** Synthesis of the *N*-benzyl-*N*-arylcyanamides using Cu/zirconium silicate nanocomposite at 75 °C<sup>a</sup>

Entry	Substrate	Product	Time (min)	Yield (%) <sup>b</sup>
1			160	86
2			160	87
3			160	87
4			175	88
5			200	84
6			175	86
7			175	88
8			130	94
9			130	92

<sup>a</sup>Reaction conditions: benzyl bromide (1.0 mmol), arylcyanamide (1.0 mmol), Cu/zirconium silicate nanocomposite (0.05 g), MeCN (7.0 ml), 75 °C.<sup>b</sup>Isolated yield.**SCHEME 3** Mechanism of the *N*-benzylation of arylcyanamides by Cu/zirconium silicate nanocomposite

(Figure 12–14). The EDS, FESEM and TEM analysis after the 5<sup>th</sup> recycle shows no substantial change in morphological characteristics and chemical compositions of the Cu/zirconium silicate nanocomposite. Thus, the as-synthesized nanocatalyst can be used successfully in consecutive reactions without remarkable loss in its catalytic performance.

## 4 | CONCLUSIONS

In the present study, a facile, efficient and direct synthesis of the various *N*-benzyl-*N*-arylcyanamides was accomplished via a copper-catalyzed reaction of arylcyanamides with benzyl bromide at 75 °C in MeCN. For the first time, the Cu/zirconium silicate nanocomposite was synthesized

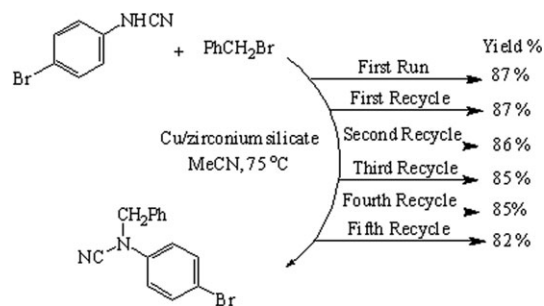


**FIGURE 11** Reusability of the Cu/zirconium silicate nanocomposite for the synthesis of *N*-benzyl-*N*-(4-bromophenyl) cyanamide

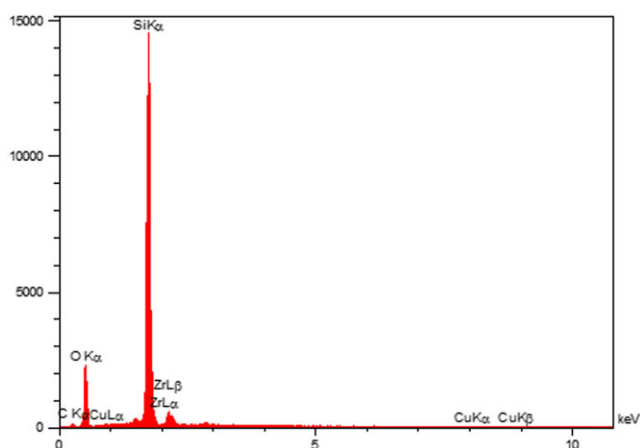


**FIGURE 12** EDS spectrum of recycled Cu/zirconium silicate nanocomposite

via reduction of  $\text{Cu}^{2+}$  ions to  $\text{Cu}^0$  in the presence of *Rubia tinctorum* leaf extract as a reducing and stabilizing agent as well as immobilization of the Cu NPs on the natural zirconium silicate surface. Indeed, we have successfully

developed an efficient method for the *N*-benzylation of arylcyanamides using Cu/zirconium silicate nanocomposite as a novel heterogeneous catalyst. This protocol showed a series of significant advantages such as operational simplicity, use of *Rubia tinctorum* leaf extract as a green source, mild reaction conditions, high product yields and thermal stability, easy availability, easy preparation and recyclability of the catalyst. The biosynthesized catalyst was easily recovered from the reaction mixture and reused with no obvious loss of its catalytic activity up to five consecutive runs.

## 5 | EXPERIMENTAL

### 5.1 | Instruments and reagents

All the reagents, materials and solvents were used without further purification in this research and purchased from the Aldrich and Merck chemical companies. Products can be characterized using different spectroscopic techniques (e.g. FT-IR,  $^1\text{H}$  and  $^{13}\text{C}$  NMR), Melting point and elemental analysis. The  $^1\text{H}$  and  $^{13}\text{C}$  NMR spectra were recorded on a Bruker (Avance DRX 300 and 400 MHz) instruments ( $\text{CDCl}_3$  or  $\text{DMSO}-d_6$  with TMS as the standard). FT-IR spectra of the synthesized samples were recorded on a Perkin-Elmer 781 spectrophotometer using pressed KBr pellets, in the  $400\text{--}4000\text{ cm}^{-1}$  range. The elemental analysis (C, H and N) was carried out on Perkin-Elmer 240c analyzer. Melting points can be determined in open capillary tubes with a BUCHI 510 melting point apparatus. Due to determination of the substrates purity and reaction progress, TLC was performed with SIL G/UV 254 silica gel plates. The crystallinity of the

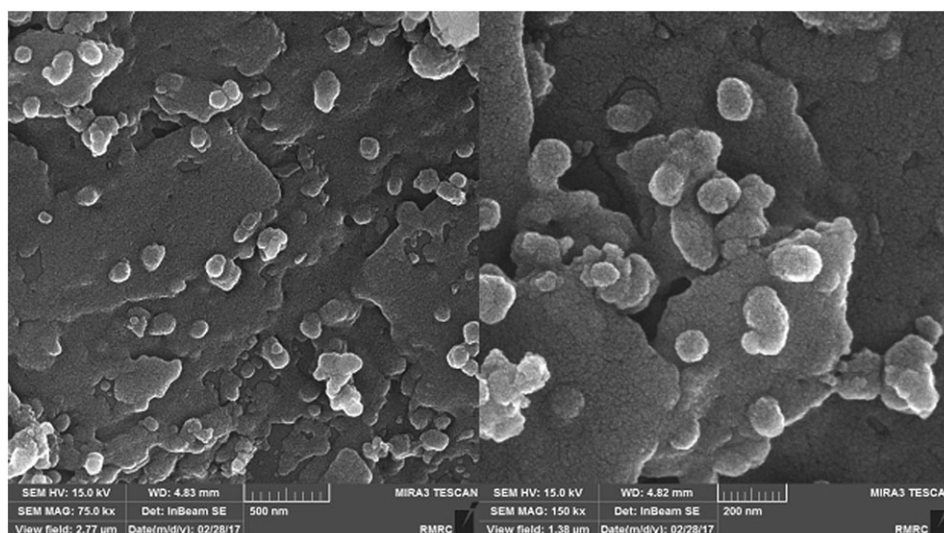


**FIGURE 13** FESEM images of recycled Cu/zirconium silicate nanocomposite

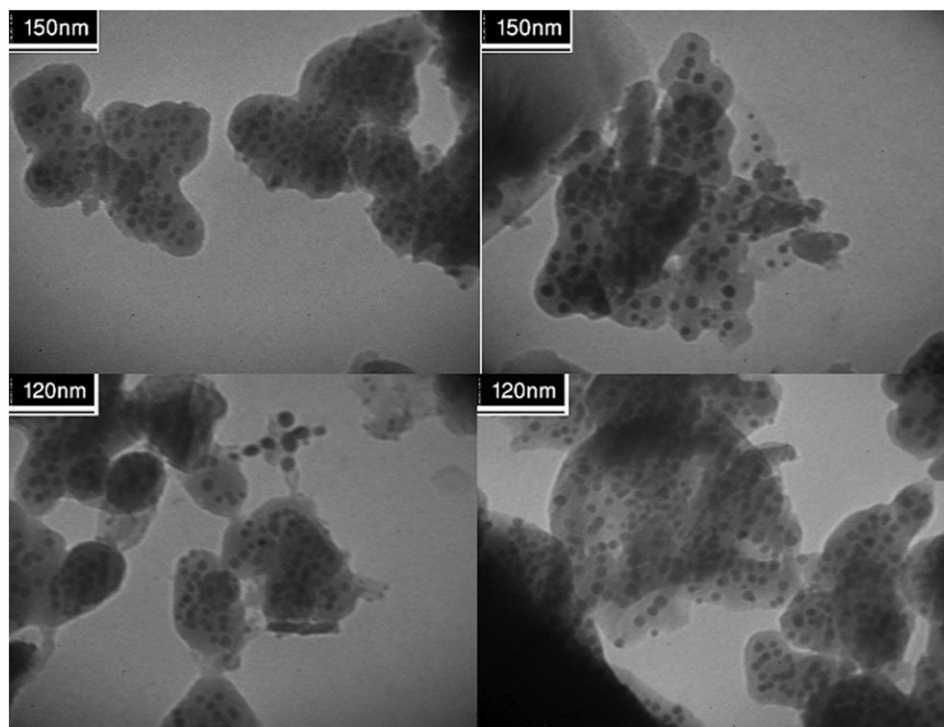


**FIGURE 14** TEM images of recycled Cu/zirconium silicate nanocomposite

nanostructures was performed on a Philips powder diffractometer type PW 1373 goniometer (using Cu K $\alpha$  radiation  $\lambda = 0.15406$  nm). The shape and size of nanostructures were determined by a field emission scanning electron microscopy (SEM micrographs) on a Hitachi S-4700 instrument and also transmission electron microscopy (TEM micrographs) were carried out with a Philips EM-208 microscope operating at an accelerating voltage of 90 kV. The EDS (Energy Dispersive X-ray Spectroscopy) data of the prepared catalyst was performed in FESEM. The Brunauer–Emmett–Teller (BET) specific surface areas (SBET) and the porosity of the sample was evaluated on the basis of nitrogen adsorption isotherms measured at 77 K using a BELSORP-max nitrogen adsorption apparatus (Japan Inc.). The sample was degassed at 150 °C before nitrogen adsorption measurements. The desorption isotherm was used to determine the pore size distribution using the Barret-Joyner-Halender (BJH) method.

## 5.2 | Preparation of *Rubia tinctorum* leaf extract

50 g of dried root powdered of the plant was added to 300 mL double distilled water and well mixed using magnetic heating stirrer at 70 °C for 30 min then filtered to obtain the extract. The obtained extract was kept at refrigerator to use further.

## 5.3 | Biosynthesis of Cu NPs using *Rubia tinctorum* leaf extract

In a 250 mL conical flask, 10 mL solution of CuCl $_2$ ·2H $_2$ O 5 mM was mixed with 100 mL of the aqueous plant extract along with vigorous shaking until gradually changing the color of the mixture during 6 min indicating the formation of Cu nanoparticles. The mixture then filtered and centrifuged at 7000 rpm for 30 min and obtained precipitation washed with absolute ethanol to remove possible impurities.

## 5.4 | Preparation of the zirconium silicate

The natural zirconium silicate used in this study originated from Isfahan area, Iran.

## 5.5 | Biosynthesis of the Cu/zirconium silicate nanocomposite using *Rubia tinctorum* leaf extract

For green synthesis of the Cu/zirconium silicate nanocomposite, a mixture containing 1.0 g of the zirconium silicate matrix and 80 mL of *Rubia tinctorum* leaf extract were stirred for 25 min at room temperature. Then, the 50 mL of 0.08 M CuCl $_2$ ·2H $_2$ O aqueous solution was gradually added into the above solution and refluxed for 4 hr at 100 °C. After ending the reaction, the obtained

Cu/zirconium silicate nanocomposite was filtered and collected by filtration, washed with distilled water three times to remove unreacted copper salts and then dried in an oven at 85 °C for 5 hr.

## 5.6 | General procedure for the *N*-benzylation of arylcyanamides using Cu/zirconium silicate nanocomposite

A mixture of arylcyanamide (1.0 mmol), benzyl bromide (1.0 mmol), Cu/zirconium silicate (0.05 g) in MeCN (7.0 mL) was taken in a flask and stirred at 75 °C for the appropriate times. The progress of the *N*-benzylation reaction was monitored by thin-layer chromatography (TLC). After completion of the reaction, the heterogeneous catalyst was recovered using of filtration, the resulting extract was concentrated, washed with water and ethanol, then dried to give pure *N*-benzylaryl cyanamides in good yields. All the synthesized products were known and characterized by using <sup>1</sup>H NMR, <sup>13</sup>C NMR, FT-IR, CHN analyses and melting points.<sup>[7]</sup> The catalyst was easily recovered by filtration, thoroughly washed with ethanol (3 × 5 mL), dried in room temperature and reused up to successive runs.

## 5.7 | Spectral data of new *N*-benzyl-*N*-aryl cyanamides

### 5.7.1 | *N*-benzyl-*N*-(4-bromophenyl) cyanamide

M.p. = 73–75 °C; FT-IR (KBr, cm<sup>-1</sup>) 3032, 2218, 1586, 1490, 1471, 1454, 1391, 1329, 1313, 1279, 1225, 1174, 1125, 1080, 1000, 821, 810, 777, 730, 696; <sup>1</sup>H NMR (300 MHz, DMSO-*d*<sub>6</sub>) δ<sub>H</sub> = 7.55 (d, *J* = 7.4 Hz, 2H), 7.40–7.33 (m, 5H), 7.16 (d, *J* = 7.4 Hz, 2H), 4.95 (s, 2H); <sup>13</sup>C NMR (75 MHz, DMSO-*d*<sub>6</sub>) δ<sub>C</sub> = 139.5, 135.1, 132.9, 129.3, 128.7, 128.3, 118.4, 115.8, 113.6, 52.5; Anal. Calcd for C<sub>14</sub>H<sub>11</sub>N<sub>2</sub>Br: C, 58.56; H, 3.86; N, 9.76. Found: C, 58.64; H, 3.93; N, 9.69.

## ACKNOWLEDGEMENTS

We gratefully acknowledge the Iranian Nano Council and the University of Qom for the support of this work.

## ORCID

Mahmoud Nasrollahzadeh  <http://orcid.org/0000-0002-4539-3544>

S. Mohammad Sajadi  <http://orcid.org/0000-0001-8284-5178>

## REFERENCES

- [1] M. Azzouz, D. Lopes, C. Courillon, M. Malacria, *Angew. Chem. Int. Ed.* **2007**, *46*, 576.
- [2] D. D. Nekrasov, *Russ. J. Org. Chem.* **2004**, *40*, 1387.
- [3] R. L. Giles, J. D. Sullivan, A. M. Steiner, R. E. Looper, *Angew. Chem. Int. Ed.* **2009**, *48*, 3116.
- [4] L.-C. Kang, X. Chen, X.-S. Wang, Y.-Z. Li, Y. Song, J.-L. Zuo, X.-Z. You, *Dalton Trans.* **2011**, *40*, 5200.
- [5] Y. Lu, C.-M. Li, Z. Wang, J. Chen, M. L. Mohler, W. Li, J. T. Dalton, D. D. Miller, *J. Med. Chem.* **2011**, 4678.
- [6] R. Kumar, D. Rai, S. K. Sharma, H. A. Saffran, R. Blush, D. L. J. Tyrrell, *J. Med. Chem.* **2001**, *44*, 3531.
- [7] D. Azarifar, F. Soleimane, F. Aliani, *J. Mol. Catal. A: Chem.* **2013**, *377*, 7.
- [8] M. Nasrollahzadeh, Y. Bayat, D. Habibi, S. Moshae, *Tetrahedron Lett.* **2009**, *50*, 4435.
- [9] R. J. Crutchley, *Coord. Chem. Rev.* **2001**, *219*, 125.
- [10] M. B. Gawande, A. Goswami, F.-X. Felpin, T. Asefa, X. Huang, R. Silva, X. Zou, R. Zboril, R. S. Varma, *Chem. Rev.* **2016**, *116*(6), 3722.
- [11] F. Gao, H. Pang, S. Xu, Q. Lu, *Chem. Commun.* **2009**, *24*, 3571.
- [12] X. Zhou, X. Huang, X. Qi, S. Wu, C. Xue, F. Boey, Q. Yan, P. Chen, H. Zhang, *J. Phys. Chem. C* **2009**, *113*, 10842.
- [13] M. Nasrollahzadeh, S. M. Sajadi, A. Hatamifard, *Appl. Catal. Environ.* **2016**, *191*, 209.
- [14] M. Trose, M. Dell'Acqua, T. Pedrazzini, V. Pirovano, E. Gallo, E. Rossi, A. Caselli, G. Abbiati, *J. Org. Chem.* **2014**, *79*, 7311.
- [15] Y. Zhang, P. Li, M. Wang, L. Wang, *J. Org. Chem.* **2009**, *74*, 4364.
- [16] K. Namitharan, K. Pitchumani, *Eur. J. Org. Chem.* **2010**, 411.
- [17] G. A. Price, A. K. Brisdon, K. R. Flower, R. G. Pritchard, P. Quayle, *Tetrahedron Lett.* **2014**, *55*, 151.
- [18] M. M. Islam, A. S. Roy, S. M. Islam, *Catal. Lett.* **2016**, *146*, 1128.
- [19] B. Mohammadi, S. M. Hosseini Jamkarani, T. A. Kamali, M. Nasrollahzadeh, A. Mohajeri, *Turk. J. Chem.* **2010**, *34*, 613.
- [20] B. K. Ghosh, S. Hazra, B. Nak, N. N. Ghosh, *Powder Technol.* **2015**, *269*, 371.
- [21] J.-R. Chiou, B.-H. Lai, K.-C. Hsu, D.-H. Chen, *J. Hazard. Mater.* **2013**, *248-249*, 394.
- [22] M. Tajbakhsh, H. Alinezhad, M. Nasrollahzadeh, T. A. Kamali, *J. Colloid Interface Sci.* **2016**, *471*, 37.
- [23] M. Sajjadi, M. Nasrollahzadeh, S. M. Sajadi, *J. Colloid Interface Sci.* **2017**, *497*, 1.
- [24] J.-H. Park, S.-K. Kim, H. S. Kim, Y. J. Cho, J. Park, K. E. Lee, C. W. Yoon, S. W. Nam, S. O. Kang, *Chem. Commun.* **2013**, *49*, 10832.
- [25] S. Naghdi, M. Sajjadi, M. Nasrollahzadeh, K. Y. Rhee, S. M. Sajadi, B. Jaleh, *J. Taiwan Inst. Chem. Eng.* **2018**, *86*, 158.
- [26] Z. Wang, L. Song, X. He, S. Wang, *Synlett* **2009**, *3*, 447.
- [27] S. Ullah, F. Ahmad, *Polym. Degrad. Stab.* **2014**, *103*, 49.
- [28] S. Hussain, S. A. Schönrichler, Y. Güzel, H. Sonderegger, G. Abel, M. Rainer, C. W. Huck, G. K. Bonn, *J. Pharm. Biomed. Anal.* **2013**, *84*, 148.



- [29] M. E. Mahmoud, G. M. Nabil, S. M. E. Mahmoud, *J. Environ. Chem. Eng.* **2015**, 3, 1320.
- [30] G. D. Wilk, R. M. Wallace, *Appl. Phys. Lett.* **2000**, 76, 112.
- [31] J. He, T. Kunitake, A. Nakao, *Chem. Mater.* **2003**, 15, 4401.
- [32] C. Noguez, *J. Phys. Chem. C* **2007**, 111, 3806.
- [33] A. Lowe, B. Sumerlin, M. Donovan, C. McCormick, *J. Amer. Chem. Soc.* **2002**, 124, 11562.
- [34] S. M. Pourmortazavi, M. Taghdiri, V. Makari, M. Rahimi-Nasrabadi, *Spectrochim. Acta a Mol. Biomol. Spectrosc.* **2015**, 136, 1249.
- [35] S. M. Pourmortazavi, M. Taghdiri, N. Samimi, M. Rahimi-Nasrabadi, *Mater. Lett.* **2014**, 121, 5.
- [36] M. Rahimi-Nasrabadi, S. M. Pourmortazavi, S. A. Sadat Shandiz, F. Ahmadi, H. Batooli, *Nat. Prod. Res.* **2014**, 28, 1964.
- [37] C. M. Cirtiu, A. F. Dunlop-Briere, A. Moores, *Green Chem.* **2011**, 13, 288.
- [38] X. Lin, M. Wu, D. Wu, S. Kuga, T. Endo, Y. Huang, *Green Chem.* **2011**, 13, 283.
- [39] B. Khodadadi, M. Bordbar, M. Nasrollahzadeh, *J. Colloid Interface Sci.* **2017**, 490, 1.
- [40] P. Banerjee, M. Satapathy, A. Mukhopahayay, P. Das, *Bioresour. Bioprocess.* **2014**, 1(3), 1.
- [41] S. Anmar Aboud, *J. Al-Nahrain Univ.* **2010**, 13, 166.
- [42] Y. B. Tripathi, M. Sharma, *Indian J. Biochem. Biophys.* **1998**, 35, 1998.
- [43] S. Sedigheh, Y. A. Zoheir, T. M. Fakhr, M. A. Hassan, *Bot. Res. Inter.* **2009**, 2, 7.
- [44] Y. X. Bao, S. X. Wang, L. J. Wu, X. Z. Li, *Chin. Qiao* **1990**, 25, 834.
- [45] M. Sharifzadeh, N. Ebadi, A. Manayi, M. Kamalinejad, H. Rezaeizadeh, M. Mirabzadeh, B. Bonakdar Yazdi, M. Khanavi, *J. Med. Plant.* **2014**, 13, 2014.
- [46] A. Fatahi Bafghi, M. T. Noorbala, S. H. Hejazzian, *World J. Zool.* **2008**, 25, 3.
- [47] Available online at; [http://khartasia-crcc.mnhn.fr/fr/common\\_names\\_fr/garance-des-teinturiers](http://khartasia-crcc.mnhn.fr/fr/common_names_fr/garance-des-teinturiers).
- [48] B. El-Gammal, S. A. Shady, *Colloids Surf., A.* **2006**, 287, 132.
- [49] A. Esmaeilifar, S. Rowshanzamir, A. Behbahani, *Iran. J. Hydr. Fuel Cell* **2014**, 3, 163.
- [50] A. Umer, S. Naveed, N. Ramzan, M. S. Rafique, M. Imran, *Revista Matéria* **2014**, 19(3), 197.

**How to cite this article:** Nasrollahzadeh M, Sajjadi M, Sajadi SM. Green synthesis of Cu/zirconium silicate nanocomposite by using *Rubia tinctorum* leaf extract and its application in the preparation of *N*-benzyl-*N*-arylcyanamides. *Appl Organometal Chem.* 2018;e4705. <https://doi.org/10.1002/aoc.4705>